Plant Physiology®

Research Article

The trajectory in catalytic evolution of Rubisco in *Posidonia* seagrass species differs from terrestrial plants

Sebastià Capó-Bauçà [iD] ,[1,*] Spencer Whitney [iD] ,[2] Concepción Iñiguez [iD] ,[1] Oscar Serrano [iD] ,[3,4] Timothy Rhodes [iD] [2] and Jeroni Galmés [iD] [1]

1   Research Group on Plant Biology under Mediterranean Conditions. Universitat de les Illes Balears-INAGEA, Palma 07122, Spain
2   Research School of Biology, Australian National University, Canberra, ACT 2601, Australia
3   Centro de Estudios Avanzados de Blanes, Consejo Superior de Investigaciones Científicas (CEAB-CISC), Blanes 17300, Spain
4   School of Science, Centre for Marine Ecosystems Research, Edith Cowan University, Joondalup, WA 6027, Australia

*Author for correspondence: sebastia.capo@uib.cat

Abstract

The CO_2-fixing enzyme Ribulose bisphosphate carboxylase-oxygenase (Rubisco) links the inorganic and organic phases of the global carbon cycle. In aquatic systems, the catalytic adaptation of algae Rubiscos has been more expansive and followed an evolutionary pathway that appears distinct to terrestrial plant Rubisco. Here, we extend this survey to differing seagrass species of the genus *Posidonia* to reveal how their disjunctive geographical distribution and diverged phylogeny, along with their CO_2 concentrating mechanisms (CCMs) effectiveness, have impacted their Rubisco kinetic properties. The Rubisco from *Posidonia* species showed lower carboxylation efficiencies and lower sensitivity to O_2 inhibition than those measured for terrestrial C_3 and C_4-plant Rubiscos. Compared with the Australian *Posidonia* species, Rubisco from the Mediterranean *Posidonia oceanica* had 1.5–2-fold lower carboxylation and oxygenation efficiencies, coinciding with effective CCMs and five Rubisco large subunit amino acid substitutions. Among the Australian *Posidonia* species, CCM effectiveness was higher in *Posidonia sinuosa* and lower in the deep-living *Posidonia angustifolia*, likely related to the 20%–35% lower Rubisco carboxylation efficiency in *P. sinuosa* and the two-fold higher Rubisco content in *P. angustifolia*. Our results suggest that the catalytic evolution of *Posidonia* Rubisco has been impacted by the low CO_2 availability and gas exchange properties of marine environments, but with contrasting Rubisco kinetics according to the time of diversification among the species. As a result, the relationships between maximum carboxylation rate and CO_2- and O_2-affinities of *Posidonia* Rubiscos follow an alternative path to that characteristic of terrestrial angiosperm Rubiscos.

Introduction

Ribulose 1,5-bisphosphate carboxylase/oxygenase (Rubisco) is the most abundant protein worldwide and it represents the key entry point of carbon into the biosphere (Bar-On and Milo, 2019). Rubisco catalyzes the initial step of the Calvin–Benson–Bassham cycle, binding CO_2 onto

ribulose-1,5-bisphosphate (RuBP) and breaking the 6-carbon intermediate into two molecules of 3-phosphoglycerate (3PGA). This carboxylation reaction is compromised by an inability to fully discriminate CO_2 from O_2, leading RuBP oxygenation by Rubisco to produce one molecule of 3PGA and one molecule of 2-phosphoglycolate (2PG) (Sage et al., 2012). The metabolic toxicity of 2PG necessitates its recycling back into 3PGA via photorespiration that consumes energy and releases previously fixed CO_2 (Bauwe et al., 2012). In terrestrial C_3 plants, the oxygenase activity of Rubisco can cause losses exceeding 25% of the CO_2 assimilated by photosynthesis, placing Rubisco as one of the prime targets for enhancing crop photosynthesis (Galmés et al., 2019).

Substantial progress has been made in the exploration of the natural Rubisco kinetic diversity, with some red algae producing Rubiscos whose improved carboxylation properties are predicted to impart a substantial impact on plant photosynthesis (Whitney et al., 2001) and also crop yield (Zhu et al., 2004). More expansive surveys of Rubisco natural kinetic variability have revealed a much broader scope in catalytic adaptation (Iñiguez et al., 2020) than the constrained adaptive landscape initially proposed (Tcherkez et al., 2006; Savir et al., 2010). Recent findings by Cummins (2021) and Bouvier et al. (2021) suggest that these perceived catalytic trade-off limitations to Rubisco catalytic potential stemmed from interpretations derived from limited, primarily terrestrial plant Rubisco, datasets that did not account for Rubisco large (RbcL) subunit phylogenies. Either way, fully appreciating the catalytic potential of Rubisco necessitates a broader exploration of its natural catalytic diversity, an undertaking that has only recently gained momentum (Young et al., 2016; Heureux et al., 2017; Iñiguez et al., 2019; Banda et al., 2020; Davidi et al., 2020; Goudet et al., 2020).

Marine environments are particularly useful in the study of the adaptive evolution of Rubisco. In seawater, CO_2 diffusion is 10,000 times slower than in air, limiting the diffusive supply of CO_2 to Rubisco. Moreover, $< 1\%$ of the dissolved inorganic carbon (DIC) is in the form of CO_2 (Maberly and Gontero, 2017), which means that the CO_2 concentration in air-equilibrated seawater is below the CO_2 semi-saturation constant reported for most Rubiscos (Iñiguez et al., 2020). These limitations in CO_2 supply for photosynthesis have been reduced by the development of CO_2 concentrating mechanisms (CCMs) in aquatic phototrophs, mostly involving the direct or indirect uptake of the most abundant DIC form, bicarbonate (Raven and Beardall, 2016). As a result, aquatic CCMs usually combine active H^+ extrusion pumps and/or bicarbonate transporters, in conjunction with carbonic anhydrases, to increase the CO_2 concentration around Rubisco active sites (known as biophysical CCMs; Badger et al., 1998; Giordano et al., 2005; Raven et al., 2017; Fei et al., 2022). In terrestrial plants, the evolution of biochemical CCMs (C_4 metabolisms) has impacted the catalytic adaptation of Rubisco (Whitney et al., 2011; Kapralov et al., 2012; Sharwood et al., 2016), but also

in C_3-species, a co-adaptation between mesophyll CO_2 conductance and Rubisco kinetics has been revealed (Galmés et al., 2017). While the co-evolutionary trends between algal Rubisco kinetics and their biophysical CCM have been previously analyzed (Goudet et al., 2020; Iñiguez et al., 2020) there is still little understanding of this co-adaptive trajectory in seagrasses (Larkum et al., 2017), the only group of angiosperms that colonized the oceans some 100 Mya (million years ago) (Hemminga and Duarte, 2000).

Seagrass meadows include $\sim$70 species belonging to 12 genera distributed across the coastal areas of all continents except Antarctica and are recognized as highly productive habitats that provide numerous ecosystem services, including carbon sequestration and ocean acidification amelioration, contributing to climate change mitigation (Duarte et al., 2013; Ricart et al., 2021). The genus *Posidonia* is one of the most relevant genera among seagrasses and contains relevant species in terms of biomass and carbon sequestration capacity (Duarte and Chiscano, 1999), being distributed in seven species along the Australian coastlines and a single *Posidonia oceanica* species endemic to the Mediterranean Sea (Campey et al., 2000). This disjunct species distribution suggests there may have been a loss of *Posidonia* species from those that originally connected the Mediterranean and Australian populations during Pangea (Larkum et al., 2006). Within these phylogenetically separate clades of *Posidonia* species it is unclear the extent to which growth habitat differences within and between both geographical locations have impacted the adaptive evolution of their CCM and Rubisco. Here, we examine the ecophysiology and Rubisco biochemistry at 25°C among the Mediterranean *P. oceanica* and four distinct lineages of *Posidonia* species from the seven morphologically described species found in Australia (Aires et al., 2011). We reveal substantial variation in the Rubisco catalytic properties of *P. oceanica* relative to the more conserved properties among the Australian species. The correlations between the slow carboxylation turnover rate, low CO_2-affinity, and high insensitivity to O_2 inhibition of *Posidonia* Rubisco follow an alternative pathway in kinetic evolution to that characteristic of terrestrial angiosperms.

Results

Rubisco kinetic traits among *Posidonia* species

The characterization of Rubisco kinetics at 25°C within the genus *Posidonia* revealed a lower Rubisco affinity for CO_2 (i.e. higher Michaelis–Menten constant for CO_2 at 0% of O_2, K_c) in the Mediterranean *P. oceanica* than in the other Australian *Posidonia* species (Table 1). The lowest Rubisco affinity for CO_2 under ambient O_2 was also observed in *P. oceanica* (K_c^{air} of $56.0 \pm 1.0\,\mu M$ in *P. oceanica* and around 25–27 μM in the Australian *Posidonia* species). In contrast, no differences were detected in the semi-saturation constant for O_2 (K_o) and in the CO_2/O_2 specificity factor ($S_{c/o}$) among all five *Posidonia* species (Table 1). The higher K_o values of all *Posidonia* Rubiscos (1,000–1,300 μM) are among

Table 1 Rubisco kinetic parameters

Species	$S_{c/o}$ (mol mol⁻¹)	K_c (µM)	K_c^{air} (µM)	K_o (µM)	k_{cat}^c (s⁻¹)	k_{cat}^c/K_c (s⁻¹ mM⁻¹)	k_{cat}^c/K_c^{air} (s⁻¹ mM⁻¹)	k_{cat}^o (s⁻¹)	k_{cat}^o/K_o (s⁻¹ mM⁻¹)
P. angustifolia	93.3 ± 1.1 a	22.0 ± 1.3 b	27.0 ± 0.1 b	1,313 ± 356 a	1.90 ± 0.11 a	87.0 ± 8.4 ab	70.4 ± 4.1 b	1.16 ± 0.22 a	0.93 ± 0.09 ab
P. australis	91.5 ± 0.9 a	21.1 ± 1.3 b	26.4 ± 0.5 b	1,142 ± 328 a	1.84 ± 0.08 a	88.1 ± 8.5 ab	69.7 ± 3.6 b	1.04 ± 0.18 a	0.96 ± 0.09 ab
P. coriacea	90.0 ± 0.8 a	20.1 ± 0.9 b	25.4 ± 0.5 b	1,139 ± 378 a	2.13 ± 0.04 a	106.5 ± 3.5 a	84.0 ± 2.0 a	1.32 ± 0.39 a	1.18 ± 0.03 a
P. sinuosa	93.1 ± 1.4 a	19.6 ± 2.5 b	25.7 ± 1.1 b	995 ± 306 a	1.41 ± 0.11 b	74.6 ± 11.6 b	55.2 ± 6.0 c	0.73 ± 0.17 a	0.80 ± 0.12 b
P. oceanica	90.1 ± 1.3 a	45.0 ± 1.8 a	56.0 ± 1.0 a	1,329 ± 179 a	2.19 ± 0.12 a	50.7 ± 3.6 c	40.4 ± 3.5 d	0.71 ± 0.11 a	0.53 ± 0.04 c
T. aestivum[1] (C₃)	91.1 ± 0.5	11.3 ± 0.3	16.1 ± 0.9	422 ± 38	3.40 ± 0.08	307.4 ± 11.9	217.2 ± 13.7	1.79 ± 0.16	4.01 ± 0.29
Z. mays[1] (C₄)	87.2 ± 2.4	25.3 ± 2.7	40.9 ± 4.7	512 ± 125	4.38 ± 0.38	225.3 ± 39.5	131.3 ± 27.2	1.06 ± 0.22	2.66 ± 0.43

Notes: Parameters shown are the Michaelis–Menten constant for CO_2 at 0% O_2 (K_c, n = 3–4) and ambient O_2 (K_c^{air}, n = 3–4), and for O_2 (K_o, n = 3–4); Rubisco CO_2/O_2 specificity ($S_{c/o}$, n = 3–4), the maximum carboxylation rate (k_{cat}^c, n = 3–4), and the maximum oxygenation rate (k_{cat}^o, n = 3–4). Values are means ± SE of n biological replicates. Different small letters show significant differences among species (P < 0.05, one-way ANOVA followed by Duncan's test or Kruskal–Wallis test followed with Bonferroni correction for nonparametric data).
[1]Data for the reference C₃ species (wheat, *T. aestivum*) and C₄ species (maize, *Z. mays*) from Iñiguez et al. (2020).

the highest ever reported for angiosperms, making them distinct outliers (especially for *P. oceanica* Rubisco) for the close linear relationship between K_c and K_o shared among terrestrial plant Rubisco (Figure 1A).

In terms of catalytic speed, the slowest carboxylation turnover rate (k_{cat}^c) was observed for *Posidonia sinuosa* Rubisco ($1.4 ± 0.1$ s⁻¹) while it was more conserved among the other *Posidonia* species ($1.8–2.2$ s⁻¹). The high K_c and K_c^{air} of *P. oceanica* Rubisco and the low k_{cat}^c of the *P. sinuosa* enzyme resulted in lower carboxylation efficiencies compared with the other species (Table 1). Notably, the correlation between k_{cat}^c and K_c for all *Posidonia* Rubiscos deviated substantially from that of C₃ and C₄ plant Rubisco (Figure 1B), resulting in seagrass Rubisco k_{cat}^c/K_c efficiencies ($51–107$ s⁻¹mM⁻¹) greater than two-fold lower than those reported for terrestrial plants (e.g. 194 and 262 s⁻¹mM⁻¹ for wheat [*Triticum aestivum*] and rice [*Oryza sativa*] Rubisco; Hermida-Carrera et al., 2016). This result suggests a different evolutionary trajectory in the catalytic adaptation of Rubisco in *Posidonia* species relative to terrestrial angiosperms. Similar oxygenation turnover rates (k_{cat}^o) were obtained among *Posidonia* species, with a significantly lower oxygenation catalytic efficiency (k_{cat}^o/K_o) observed for *P. oceanica* Rubisco (Table 1).

The lower CO_2 affinity of *P. oceanica* Rubisco may arise from differences in the RbcL sequence

The *Posidonia* phylogenetic tree derived from nuclear rRNA-ITS region mapping revealed that the Mediterranean *P. oceanica* species diverged 68 Mya from its Australian relatives, consistent with their differing geographical distribution (Figure 2A). Accompanying this evolutionary divergence, the RbcL of *P. oceanica* showed five amino acid differences relative to the shared RbcL sequence by each Australian *Posidonia* species (Figure 2B). Taking into account the location of these five residues in the holoenzyme complex (Figure 2C) and their structural and reported catalytic impacts (Supplemental Table S1), it is conceivable the Thr-279-Ser or/and Ser-449-Thr substitutions in *P. oceanica* Rubisco might account for its reduced affinity for CO_2 (i.e. higher K_c). The shared RbcL sequence among the Australian
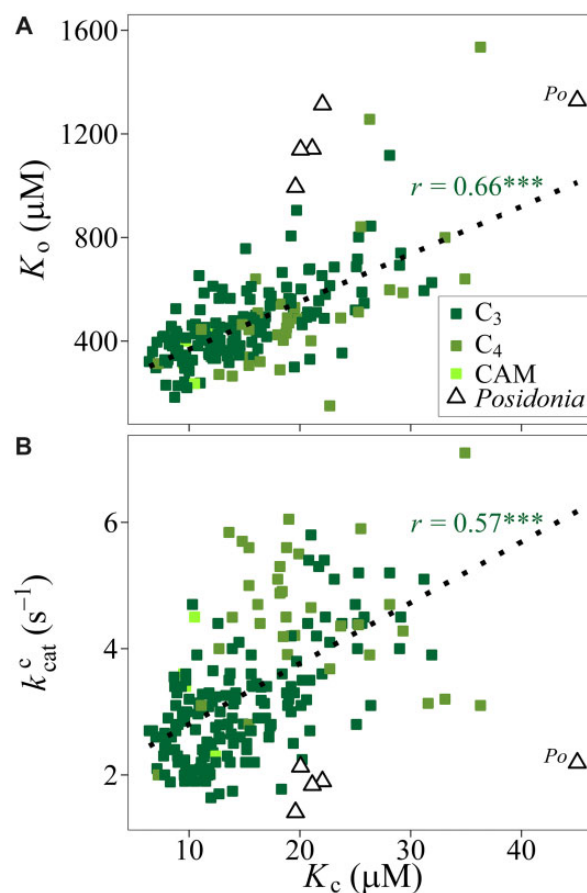

Figure 1 Diversity in the catalytic properties of *Posidonia* Rubisco relative to C₃, C₄, and CAM plants. A, Correlation between the Michaelis–Menten constant for CO_2 (K_c) and the Michaelis–Menten constant for O_2 (K_o); (B) and between K_c and the maximum carboxylation rate (k_{cat}^c). Empty triangles are the species of *Posidonia* measured in this study (n = 5) and *Po* indicates the Mediterranean endemic *P. oceanica*. Light and dark green squares belongs to terrestrial plants compiled by Iñiguez et al. (2020) (n = 178 in A and 203 in B). r is the reported Pearson's regression coefficient of terrestrial plants and asterisks show the significance of the correlation test (***P < 0.001).

Posidonia species, however, suggest that the low k_{cat}^c of *P. sinuosa* Rubisco likely arise from differences in its RbcS sequence(s).
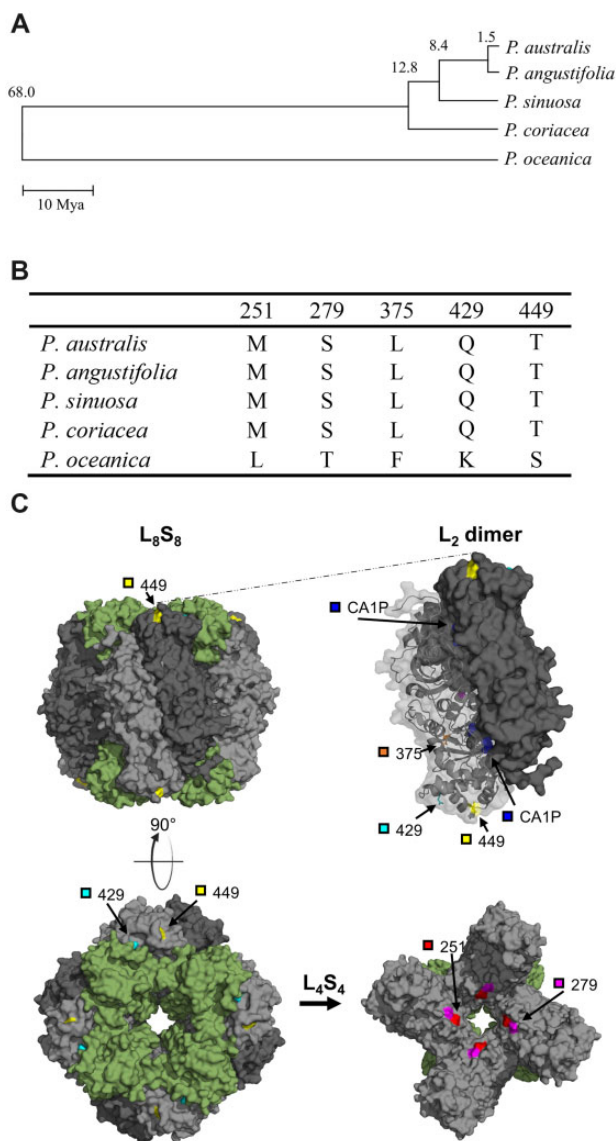
Figure 2 Phylogenetic and Rubisco molecular diversity across *Posidonia* species. A, Phylogenetic tree of *Posidonia* species analyzed in the study abbreviated from that derived by Aires et al. (2011) from mapping the rRNA-internal transcribed spacer (ITS) region; numbers above branches are the divergence dates (in Mya) estimated on the maximum-likelihood topology derived from the ITS data set; B, amino acid changes among *rbcL* of *Posidonia* species; C, location of the variable amino acid positions of *P. oceanica* RbcL mapped onto the crystal structure of spinach Rubisco (8RUC) using Pymol V1.8.x. Residues 251, 279, 375, 429, and 449, and the inhibitor CA1P are highlighted.

CCMs operate at differing effectiveness among *Posidonia* species

The in vivo photosynthetic responses to CO_2 were determined either in a nonbuffered seawater or Tris-buffered seawater. As a result, we obtained two in vivo Michaelis–Menten constant measures of photosynthetic affinity for CO_2 (K_m and $K_{m\text{-Tris}}$) and for DIC ($K_{m\ DIC}$ and $K_{m\text{-Tris}\ DIC}$). The $K_{m\text{-Tris}}$ was significantly higher than K_m for each *Posidonia* species, as well as the $K_{m\text{-Tris}\ DIC}$ relative to $K_{m\text{-DIC}}$

(Figure 3 and Supplemental Table S2). These results demonstrate that the in vivo photosynthetic affinity for both CO_2 and DIC decreased when the seawater pH is buffered, suggesting the presence of CCMs associated with active H^+ extrusion pumps in all *Posidonia* species. The K_m and $K_{m\ DIC}$ were highest in *Posidonia angustifolia* (K_m of $80 \pm 6\ \mu M$ of CO_2 and $K_{m\ DIC}$ of $11 \pm 1\ mM$ of HCO_3^-), also showing the lowest ratio $K_{m\text{-Tris}}/K_m$ (Figure 3). These findings suggest a less effective CCM in this species.

To determine the capacity of CCMs to concentrate CO_2 near the active site of Rubisco, the Rubisco response to CO_2 (in vitro CO_2 assimilation) under ambient O_2 was compared with the in vivo photosynthetic CO_2 response in nonbuffered seawater. Except for *P. angustifolia*, the photosynthetic response measured in vivo was higher than the in vitro rates simulated (Figure 3), consistent with the presence of a CCM able to concentrate CO_2 around Rubisco and sustain the higher photosynthetic rates observed in vivo. When buffered with Tris, the in vivo rates of CO_2 assimilation were substantially lower (Figure 3), suggesting the rates of photosynthesis in all *Posidonia* species were limited by mesophyll CO_2 diffusion when CCM was inhibited.

In aquatic organisms, the supply of CO_2 decreases along the diffusion pathway to Rubisco due to the boundary layer, cell wall, and lipidic membranes. A K_c^{air}/K_m ratio > 2.5 is therefore associated with the presence of an effective CO_2 concentration around Rubisco in aquatic organisms (Raven et al., 2017). On this basis, only *P. oceanica* and *P. sinuosa* appear to effectively concentrate CO_2 near the Rubisco active sites (Figure 3), while in the other *Posidonia* species, the CCMs appear less effective in ameliorating the mesophyll-associated restrictions to CO_2 diffusion, especially in *Posidonia coriacea* and *P. angustifolia* that show the lowest $K_c^{air}/K_{m\text{-Tris}}$ ratio (Figure 3). In terms of maximum in vivo photosynthetic rates ($A_{n\ max}$) expressed in terms of leaf area, biomass, or chlorophyll content, the highest values were found in *P. angustifolia*, *Posidonia australis*, and *P. sinuosa* and the lowest in *P. coriacea* and *P. oceanica* (Supplemental Table S2).

Chlorophyll and Rubisco contents are higher in *P. angustifolia*

Higher content of chlorophyll *a* and *b*, carotenoids, and total soluble protein (TSP) was found in the leaves of *P. angustifolia* (Figure 4A and Supplemental Table S3). This result suggests higher photosystem I and photosystem II contents in this species, consistent with a requirement for higher resource investment into light capture by the species in response to its deeper habitat (Supplemental Table S4). The Rubisco content in this species (as a percent of TSP) was also the highest (Figure 4B and Supplemental Table S3) probably to maintain suitable rates of CO_2-assimilation in response to lower CCM activity. Overall, however, all *Posidonia* species produced relatively low amounts of Rubisco (4%–7% w/w of the TSP), greater than three-fold less than that produced in terrestrial plants ($> 20\%$ w/w
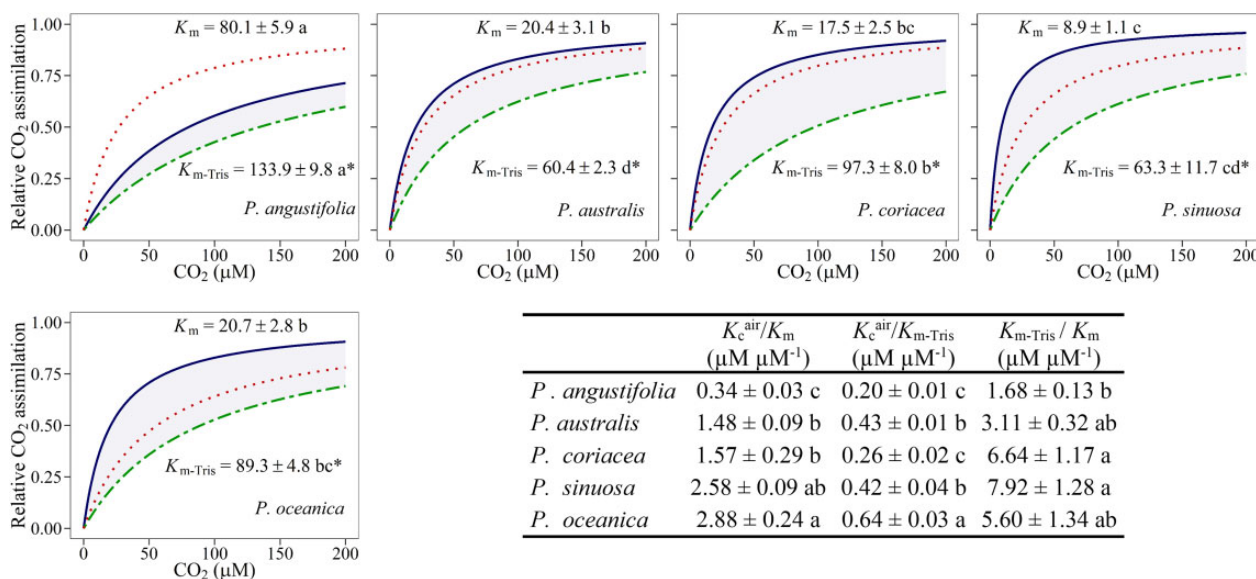
	K_c^{air}/K_m (μM μM^{-1})	$K_c^{air}/K_{m\text{-}Tris}$ (μM μM^{-1})	$K_{m\text{-}Tris}/K_m$ (μM μM^{-1})
P. angustifolia	0.34 ± 0.03 c	0.20 ± 0.01 c	1.68 ± 0.13 b
P. australis	1.48 ± 0.09 b	0.43 ± 0.01 b	3.11 ± 0.32 ab
P. coriacea	1.57 ± 0.29 b	0.26 ± 0.02 c	6.64 ± 1.17 a
P. sinuosa	2.58 ± 0.09 ab	0.42 ± 0.04 b	7.92 ± 1.28 a
P. oceanica	2.88 ± 0.24 a	0.64 ± 0.03 a	5.60 ± 1.34 ab

Figure 3 Relative CO_2 assimilation of photosynthesis in vivo (solid line), photosynthesis in vivo inhibited by Tris-Buffer (dashed line) and in vitro Rubisco relative CO_2 assimilation under air conditions (dotted line). Parameters plotted are the Michaelis–Menten constant for CO_2 of photosynthesis in vivo (K_m, $n = 4$), the Michaelis–Menten constant for CO_2 of photosynthesis in vivo inhibited by Tris-buffer ($K_{m\text{-}Tris}$, $n = 4$), and the Michaelis–Menten constant for CO_2 at 21% O_2 of Rubisco in vitro (K_c^{air}, $n = 3–4$). Maximum CO_2 assimilation was standardized to 1 for comparative purposes. Values plotted are means ± SE of n biological replicates. Different small letters show significant differences among species ($P < 0.05$, one-way ANOVA followed by Duncan's test or Kruskal–Wallis test followed with Bonferroni correction for nonparametric data) and letters with * indicate significant differences between K_m and $K_{m\text{-}Tris}$ ($P < 0.05$, Student's t test or Mann–Whitney' test for nonparametric data).

TSP; Galmés et al., 2014b). Notably, the leaf N content also differed among the *Posidonia* species, with significantly higher amounts in *P. oceanica*, *P. australis*, and *P. sinuosa* (Supplemental Table S3).

Discussion

Globally, the seagrass genus *Posidonia* is distributed asymmetrically with seven species localized along Australian coastlines and one, *P. oceanica*, endemic to the Mediterranean Sea. Consistent with its disjunct geographic location and phylogenetic divergence, the RbcL in *P. oceanica* contained five unique amino acid substitutions that may possibly account for its lower CO_2-affinity and carboxylation efficiency relative to Rubisco from the four Australian *Posidonia* species studied (Table 1). This phylogenetically related and distinctively Rubisco kinetic properties of *P. oceanica* might be associated with its effective CCMs, only comparable with the CCMs of the Australian *P. sinuosa* (Figure 3). The high effectiveness of CCMs in *P. sinuosa* is possibly related to its low k_{cat}^c and Rubisco carboxylation efficiency under ambient O_2, being significantly different from the other Australian *Posidonia* species possessing the same RbcL sequence (Table 1 and Figure 2), and hence, suggesting a possible coadaptation of the Rubisco kinetic properties with CCMs among Australian *Posidonia* species. Compared with terrestrial plant Rubiscos, k_{cat}^c and affinities for both CO_2 and O_2 of all *Posidonia* Rubisco isoforms were significantly impaired (Table 1) and diverged from that conserved among C_3- and C_4-terrestrial plant species (Figure 1), leading to much lower carboxylation efficiencies and thus,

demonstrating that *Posidonia* Rubisco has evolved on an alternative trajectory to terrestrial plants.

The impact of RbcL sequence variation on *Posidonia* Rubisco catalysis

The majority of Form I Rubisco mutagenic studies have focused on changes to the RbcL subunits that assemble as dimers to form a holoenzyme octameric core that houses the eight catalytic sites (Aigner et al., 2017). Indeed, the Met-309-Ile RbcL substitution has been biochemically shown to impart the catalytic switch between C_3 and C_4 kinetics among *Flaveria* Rubisco (Whitney et al., 2011) with an additional kinetic role for residue 328 hypothesized for *Limonium* Rubisco (Galmés et al., 2014a). Phylogenetic reconstruction analyses with Solanaceae Rubisco have also identified sub-sets of RbcL mutations (that include within them S279T, K429Q, and C449S substitutions) that can positively impact tobacco (*Nicotiana tabacum*) Rubisco catalysis (Lin et al., 2022). Notably, the K429Q and C449G substitutions alone impair tobacco Rubisco k_{cat}^c 20% and 40%, respectively, and with undetermined impact on their affinities or specificity for CO_2 and O_2 (Lin et al., 2021). The conserved k_{cat}^c among *P. oceanica* and most Australian *Posidonia* Rubisco isoforms would suggest the RbcL Q429K and T449S substitutions in *P. oceanica* do not impact maximum CO_2-fixation rate (Table 1). More likely, changes to RbcL residue 375 might have greater catalytic impact given its nearby locality to A378, a conserved residue within a hydrophobic region near the active site. Mutation of A378 is invariably catalytically detrimental, and only an A378V
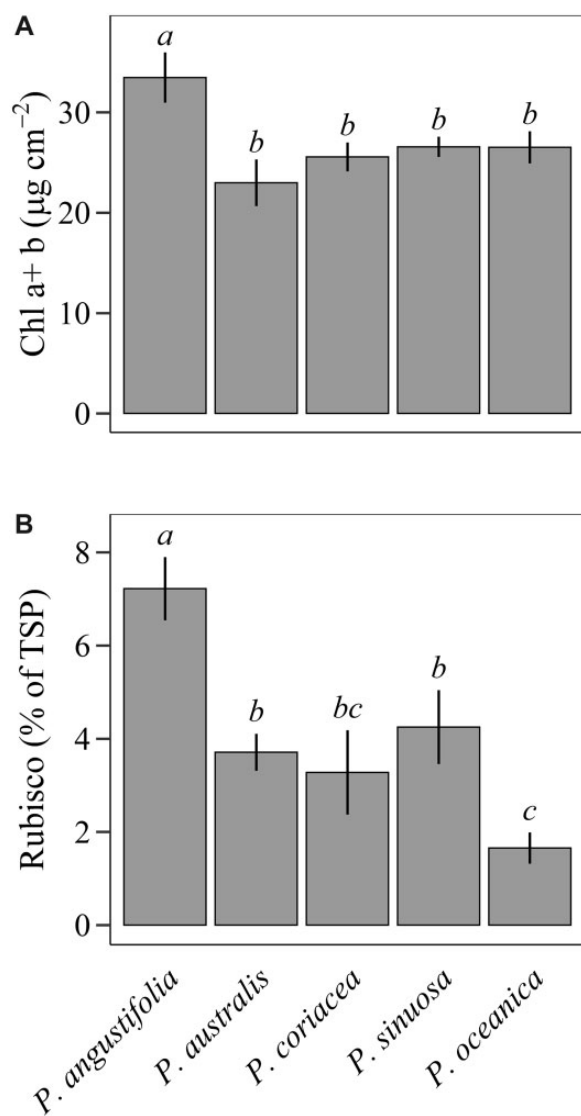
Figure 4 Biochemical leaf parameters. A, Total chlorophyll leaf content (Chl$_{a+b}$, $n = 4$); B, Rubisco content (% of TSP, $n = 6$). Values are means ± SE of n biological replicates. Different small letters show significant differences among species ($P < 0.05$, one-way ANOVA followed by Duncan's test or Kruskal–Wallis test followed with Bonferroni correction for nonparametric data). For comparative purposes, we provide the total chlorophyll and Rubisco leaf content of wheat (reference C$_3$ plant): Chl$_{a+b}$ = 29.1 ± 1.2 µg cm^{-2} (Kiani-Pouya and Rasouli, 2014) and Rubisco content = 28% ± 1% of TSP (Galmés et al., 2014b); and maize (reference C$_4$ plant): Chl$_{a+b}$ = 44 ± 1.7 µg cm^{-2} (Lagriffoul et al., 1998) and Rubisco content = 7.4% ± 1% of TSP (Sharwood et al., 2014).

mutation in cyanobacteria Rubisco has been shown to produce a functional, though nine-fold lower k_{cat}^{c}, enzyme (Satagopan et al., 2019). Of uncertain catalytic impact is also the co-localized RbcL residues 251 and 279 at the interface between adjoining RbcL dimers and RbcS (Figure 2C), a region shown to impact the thermal stability and catalytic efficiency of *Chlamydomonas* Rubisco (Du and Spreitzer, 2000; Spreitzer et al., 2005). The extent to which the L375F, M251L, and S279T substitutions might singly or in

combination account for the lower CO$_2$ affinity of *P. oceanica* Rubisco catalysis is unknown. The discovery of the ancillary proteins needed to produce Arabidopsis Rubisco in *Escherichia coli* (Aigner et al., 2017) may, however, provide an experimental means for mutagenic testing of *Posidonia* Rubisco catalysis—assuming there is sufficient complementarity between the chaperone folding requirements of *Posidonia* and Arabidopsis Rubisco.

While the RbcS does not directly contribute residues to the active sites in Rubisco (Figure 2C), it has long been postulated to impact holoenzyme biogenesis, stability, and catalysis (reviewed in Mao et al., 2022). This is now supported by a growing body of evidence confirming the pervasive effect heterologous RbcS can have on plant Rubisco kinetics (Ishikawa et al., 2011; Morita et al., 2014; Matsumura et al., 2020) and the impact specific RbcS amino acid changes can have on both holoenzyme assembly and catalysis (Martin-Avila et al., 2020; Lin et al., 2022). As the RbcL sequence of all four Australian *Posidonia* species is conserved (Figure 2B), we hypothesize the lower k_{cat}^{c} of *P. sinuosa* Rubisco stem from differences in RbcS sequence. Attempts to examine this by comparative RbcS transcriptome analysis have, however, proved unsuccessful due to challenges in obtaining RNA of sufficient quality.

The carboxylation and oxygenation properties of *Posidonia* Rubisco are atypical

The carboxylation efficiency of *Posidonia* Rubisco under both anoxia (k_{cat}^{c}/K_c) and ambient O$_2$ (k_{cat}^{c}/K_c^{air}) appears highly compromised relative to other angiosperms (Figure 1B). The impaired efficiency was most notable in *P. oceanica* and *P. sinuosa* (Table 1) that correspondingly appear to have more effective CCMs (Figure 3), suggesting a correlative link between Rubisco CO$_2$-supply and its kinetic adaptation. Their kinetic adaptation, however, contrasts with that of C$_4$-plant Rubisco where the CCM has facilitated the selection of improvements in k_{cat}^{c}, not the comparatively greater than two-fold slower k_{cat}^{c} of all *Posidonia* Rubiscos (Figure 1B). Accompanying the increases in C$_4$-Rubisco k_{cat}^{c} are reductions in CO$_2$ affinity (i.e. increases in K_c), a mechanistic consequence of limited physiological impact since the C$_4$-bundlesheath chloroplasts provide Rubisco with near CO$_2$ saturating levels under which to operate. This mechanistic trade-off between k_{cat}^{c} and K_c follows a linear response that is relatively well conserved among C$_3$ and C$_4$ plants (Figure 1B; Tcherkez et al., 2006; Savir et al., 2010), possibly due to their common RbcL phylogenies (Bouvier et al., 2021). Importantly, the correlation has no biological relevance since it omits consideration of each Rubiscos K_o (i.e. the extent to which their carboxylation is differentially impacted by O$_2$ inhibition). Fortuitously, a strong linear association is maintained when comparing the k_{cat}^{c} and K_c^{air} (a measure of CO$_2$ affinity in the presence of ambient O$_2$) of terrestrial plant Rubisco (Sharwood et al., 2016).

The k_{cat}^{c}–K_c correlation of *Posidonia* Rubisco possess a distinct evolutive trajectory to plant Rubiscos as its slower

turnover rates are atypically accompanied by poorer CO_2 affinities (Figure 1B). Of functional benefit, however, are corresponding reductions in O_2 affinity observed in all *Posidonia* Rubiscos (Table 1), especially in aquatic environments where photosynthetically produced O_2 diffusion out of the leaf is severely impaired. As summarized in Figure 1A, the high K_o shared by each *Posidonia* enzyme substantially exceeds those of their terrestrial counterparts and diverges from the linear K_c–K_o relationship shared among CAM, C_3, and C_4 plant Rubisco (Hermida-Carrera et al., 2016; Orr et al., 2016). Taken together, our kinetic data suggest that the coevolution of Rubisco kinetics and CCMs in *Posidonia* species is distinct to that observed in terrestrial angiosperms, which questions kinetic trade-off inferences made from phylogenetically limited kinetic datasets (Tcherkez et al., 2006; Savir et al., 2010). This finding is congruent with recent discoveries revealing that the kinetics of Form I "red"-lineage Rubiscos of CCM containing nongreen micro-algae (Young et al., 2016; Heureux et al., 2017), macroalgae (Iñiguez et al., 2019), and streptophyte green algae (Goudet et al., 2020) have evolved along differing trajectories to land plants. Indeed, it showcases that the carboxylation properties of plant Rubisco can be improved (Flamholz et al., 2019), as recently demonstrated (Lin et al., 2022).

Regulation of CCMs activity by the abiotic environment of *Posidonia* species

Understanding the genetic, metabolic, and physiological drivers underpinning the natural process of Rubisco kinetic evolution are critical to help improving our understanding of Rubisco catalysis. In the context of *Posidonia* species, they presented a low growth rate compared with terrestrial plants. For example, *P. oceanica* can grow at 2.4 g dry weight m^{-2} day^{-1} (Duarte and Chiscano, 1999), whereas terrestrial crop plants like *Sorghum* can growth at 8–15 g dry weight m^{-2} day^{-1} (Gerlach and Cottier, 1974). Nevertheless, *P. oceanica* is comparatively longer-lived and considered a highly productive species capable of storing the largest sediment organic carbon stocks reported for seagrasses (Duarte and Chiscano, 1999; Lavery et al., 2013; Mazarrasa et al., 2017). The carbon sequestration levels of *P. oceanica* are 21- to 34-fold higher than *P. sinuosa* (Serrano et al., 2014) and three-fold higher that *P. australis* (Serrano et al., 2016). Contributing to this, longer periods of sustained optimal growth conditions (light, temperature, and nutrient availability) in the Mediterranean Sea (not discernable from the averaged parameters in Supplemental Table S4) might potentially expose *P. oceanica* to higher levels of photosynthetic O_2 production for a more prolonged time. As previously reported, O_2 levels in the mesophyll cells of seagrasses can increase up to 35% above ambient levels during photosynthesis (Roberts and Moriarty, 1987; Kim et al., 2018), depending on its mesophilic resistance to gas diffusion out of the leaf. Indeed, it is hypothesized that chloroplast O_2 concentrations may also impact the catalytic evolution of Rubisco in aquatic organisms (Griffiths et al., 2017), possibly

accounting for the advantageous lower oxygenation efficiency (k_{cat}^o/K_o) of *P. oceanica* Rubisco. Testing such hypothesis requires more expansive and comparative analyses of the seasonal photosynthetic responses and Rubisco temperature–response kinetics across *Posidonia* species, as well as their mesophilic resistance to gas diffusion.

Evidence was found for the involvement of H^+ extrusion pumps in the CCMs of *Posidonia* species except for *P. angustifolia*, whose photosynthesis showed little inhibition by Tris pH buffer (see K_{m-Tris}/K_m ratio in Figure 3). Tris pH buffer competes for H^+ in the apoplast, dissipating the acidic zone generated by proton extrusion pumps in the periplasmatic space, which are required for the function of seagrass CCMs (Price and Badger, 1985). *Posidonia angustifolia* was also least effective at concentrating CO_2 near Rubisco (as signified by its greater than five-fold lower K_c^{air}/K_m ratio than the observed in other *Posidonia* species, Figure 3), suggesting that carbon acquisition in *P. angustifolia* is more reliant on diffusive supply of CO_2. Notably, the habitat of *P. angustifolia* is much deeper in the water column (20 m versus 2 m for the other species, Supplemental Table S4), where reductions in light levels may limit photosynthesis and the rate of energy production needed to fuel CCMs (Raven and Beardall, 2014, 2016). The low CCM activity in *P. angustifolia* may constitute an adaptative advantage that allows the survival of this seagrass to the lower light and higher CO_2 partial pressures deeper in the ocean column (Duarte, 1991). In support of this, the light harvesting pigment contents (chlorophyll *a*, *b* and total carotenoids) were highest in *P. angustifolia* (Supplemental Table S3), suggestive of an adaptive response to low light environments which elevates its light harvesting capacity.

Similarly, *P. angustifolia* invests a near two-fold higher proportion of their soluble protein into Rubisco (Figure 4), a response associated to the low, if any, capacity to alleviate the resistance of CO_2 diffusion by anatomical barriers. While these higher investments in Rubisco and light harvesting pigment contents did not lead to an improvement in the leaf N content of *P. angustifolia* (Supplemental Table S3), further analysis is needed to evaluate how differences in nutrient availability, growth rate, herbivory, and light availability impact the cellular biochemistry and carbon assimilation physiology of *Posidonia* species along water depth gradients, as well as the impact of these environmental variables in the oligotrophic Mediterranean waters (Fourqurean et al., 2007; Agawin et al., 2016; Garcias-Bonet et al., 2019).

Concluding remarks

This study revealed differences in the kinetic evolution of Rubisco among *Posidonia* species consistent with their disjunct geographic distribution and phylogenetic divergence, leading to five unique amino acid substitutions in the RbcL of *P. oceanica* that possibly account for its two-fold poorer Rubisco CO_2-affinity. Among Australian *Posidonia* species, we can attribute some of the Rubisco kinetics and quantity variation with differences in their CCM efficiency, as the 40% slower k_{cat}^c and 20%–35% lower carboxylation

efficiency in *P. sinuosa* or the two-fold higher Rubisco content in the deep-living *P. angustifolia*. However, further refined experiments are needed to accurately map evidence of correlations in the adaptive evolution of *Posidonia* Rubisco kinetics and their photosynthetic adaptation. Such analyses necessitate an assessment of the contrasting temperature, nutrient, CO_2 concentration, and irradiance characteristics of the habitats of each species, as well as an appreciation of their adaptive Rubisco temperature kinetic response and intracellular O_2 concentration. Nevertheless, the distinctly slower k_{cat}^c, lower CO_2 and O_2 affinities, and lower carboxylation efficiency shared by *Posidonia* Rubiscos compared with those of their distant terrestrial angiosperm relatives show how the enzyme in these seagrasses have clearly followed an alternative pathway in their kinetic evolution.

Materials and methods

Plant material

The analyzed *Posidonia* species were selected in accordance with the lineages differentiated by rRNA-ITS (Aires et al., 2011). *Posidonia australis*, *P. sinuosa*, *P. coriacea*, and *P. angustifolia* were sampled in August 2019 at Cockburn Sound (Perth, Western Australia) and the Mediterranean *P. oceanica* was collected in June 2020 at Son Verí (Mallorca, Spain). The physicochemical characteristics of the seawater, the depth, and the cardinal points at the site of collection are listed in Supplemental Table S4. Plants were maintained in aquariums at 25°C for up to 2 weeks under an irradiance of ~100 µmol photons m^{-2} s^{-1} at a photoperiod 12:12 light:darkness with filtered natural seawater replaced every 2–3 days. Healthy, epiphyte-free leaves (typically the second or third youngest leaf of the shoot) were selected for all analyses, frozen in liquid nitrogen, and stored at −80°C for biochemical analysis.

Photosynthesis versus DIC curves (P–C curves)

Net photosynthesis-DIC curves (P–C curves) were determined at 25°C by O_2 evolution measurements, using Clark type oxygen electrode chambers (Oxygraph, Hansatech, King's Lynn, UK). Leaf pieces (20–30 mg fresh weight) were placed in 2 mL of DIC-free natural seawater, obtained as described by Invers et al. (2001). O_2 evolution was measured under saturating irradiance (600 µmol photons m^{-2} s^{-1}) provided by white light LED lamps. To prevent O_2 oversaturation during the measurements, N_2 gas was bubbled into the chamber to reduce the seawater O_2 levels to ~70% ambient O_2 saturation. Oxygen saturation in air-equilibrated water was determined using the software DOTABLES (https://water.usgs.gov/software/DOTABLES/).

After stabilizing O_2 evolution rate close to zero in DIC-free seawater for 10–15 min, two photosynthesis-DIC curves were applied consecutively to each piece of leaf. The first curve was performed with nonbuffered seawater, adjusting the duration of the measurements to ensure that seawater pH varied <0.2 units. The second curve was measured in 20 mM Tris-buffered seawater (pH = 8.1). P–C curves were

measured by adding 8–12 successive aliquots of a 300-mM $NaHCO_3$ stock to obtain final DIC concentrations ranging from 0 to 20 mM in the O_2 chamber. For each DIC concentration, oxygen evolution rate was recorded for 3–5 min after rate stabilization, using the O2view software (version 2.10, Hansatech). The dissolved CO_2 concentration of each point was calculated using the CO2sys software (Lewis and Wallace, 1998) and both, the nonbuffered and Tris-buffered P–C curves, were fitted to the Michaelis–Menten function to extrapolate the net maximum photosynthetic rate (A_{max}) and the in vivo semi-saturation constant for CO_2 (K_m and K_{m-Tris}, respectively) and DIC ($K_{m\ DIC}$ and $K_{m\ DIC-Tris}$, respectively). Comparison of the result obtained for the nonbuffered and Tris-buffered P–C curves was used as a proxy for the presence and effectiveness of the CCM, as pH buffers are among the strongest inhibitors of the CCMs present in seagrasses (Larkum et al., 2017). A_{max} was normalized relative to the leaf area. The leaf area was quantified using ImageJ analysis (Wayne Rasband National Institutes of Health, USA).

TSP, Rubisco, chlorophyll, and nitrogen concentration in leaves

Frozen leaf samples were ground to a fine powder with liquid N_2 in a prechilled mortar and homogenized in 0.5 mL of extraction buffer (100 mM EPPS pH 8.0, 1 mM EDTA, 20 mM MgCl, 20 mM HCO_3^-, 10 mM dithiothreitol, 2% v/v plant protease inhibitor cocktail [P9599, Merck, USA], 4 mM phenylmethylsulfonyl fluoride, and 1% v/v triton X-100). The homogenate was centrifuged at 15,000 g for 2 min at 4°C and the supernatant used to determine the protein content and Rubisco concentration by [^{14}C]-CABP binding chromatography as described by Whitney and Sharwood (2014).

The same pieces of leaves used in the P–C curve were frozen in liquid N_2, stored at −80°C, ground in liquid N_2 in a prechilled mortar and homogenized in 0.5 mL 96% pure ethanol, centrifuged (15,000 g, 2 min, 4°C), and the solubilized photosynthetic pigment content quantified spectrophotometrically according to Lichtenthaler and Wellburn (1983). N leaf content was measured in leaf samples dried at 70°C for 72 h using an elemental analyzer (Thermo Flash EA 1112 Series, Bremen, Germany) and mass spectrometer (Thermo-Finnigan Delta XP, Bremen).

Rubisco catalytic measurements

Frozen leaf tissue (0.2–0.3 g fresh weight) was homogenized in a prechilled mortar containing an equivalent mass (0.2–0.3 g) of polyvinylpyrrolidone (PVPP) and 2 mL ice-cold extraction buffer. The homogenate was centrifuged (2 min, 15,000 g, 4°C) and aliquots of the supernatant taken for [^{14}C]-CABP binding or mixed with an equal volume of reaction buffer (100 mM EPPES-NaOH, pH 8.05, 20 mM MgCl$_2$, and 1 mM EDTA) containing 20 mM NaH^{14}CO$_3$. Following incubation at 25°C for 8–12 min (technical repeats) to ensure full Rubisco activation and no loss in activity between time points, 20 µL aliquots were used to initiate $^{14}CO_2$ fixation assays performed in 7.7 mL of septum-capped

scintillation vials containing 0.5 mL of reaction as described ([Sharwood et al., 2016](#)). The assays were performed at 25°C in reactions equilibrated with 0%, 15%, 20%, 30%, or 40% O_2 (v/v) mixed with N_2 using Wostoff gas mixing pumps with five concentrations of $^{14}CO_2$ tested at each $[O_2]$ that ranged from 6–56 µM $^{14}CO_2$ in assays at 0% v/v O_2 to 12–107 µM $^{14}CO_2$ in assays at 40% v/v O_2. The data were fitted to the Michaelis–Menten equation to derive the K_m for CO_2 (K_c) and maximal carboxylation rate (V_{max}^c) at each $[O_2]$ of Rubisco. For each biological replicate, the Michaelis–Menten constant for O_2 (K_o) was calculated using linear regression based on the values of K_c measured under the different O_2 concentrations. The carboxylation turnover rate (k_{cat}^c) was calculated by dividing V_{max}^c by the number of Rubisco catalytic sites quantified by [^{14}C]-2-CABP binding.

For $S_{c/o}$, 2.5–3 g of fresh leaf tissue was homogenized in a prechilled mortar with 25 mL of ice-cold extraction buffer mixed with PVPP to the same leaf weight. After centrifugation (10 min, 15,000 g, 4°C), the supernatant was applied to a 5-mL Mini-Macroprep High-Q strong anion-exchange cartridge (Bio-Rad, Hercules, California, USA) followed by a Superdex 200 (GE Life Sciences, Chicago, Illinois, USA) size exclusion column chromatography as described by [Sharwood et al. (2008)](#). The purified Rubisco was concentrated ~10-fold using Amicon Ultra 4 (Z740198; Merck, Kenilworth, New Jersey, USA) and used to measure $S_{c/o}$ at 25°C as described by [Kane et al. (1994)](#) in reactions equilibrated with 0.05% (v/v) CO_2 and 99.95% (v/v) O_2 mixed using Wostoff gas mixing pumps.

rbcL amplification, sequencing, and RbcL alignment

Total genomic DNA was extracted from ~10 mg of tissue using the DNeasy Plant Mini Kit (Qiagen, Hilden, Germany) and used to PCR amplify ~1,600 bp of plastome sequencing spanning the entire *rbc*L gene with primers Pos-rbcL-forward (5'-TA<u>CGTCTCTCATA</u>CATRTCGAGTAGACCTTGT-3') and Pos-rbcL-reverse (5'- TACGTCTCTTCGAAAAAGATTGGGCC GAGTTTAATT-3') using Phusion High-Fidelity DNA Polymerase. The amplified products were cloned into the *Esp3I* (restriction site in primers underlined) of vector pBP-ORF-GFP (Addgene plasmid, Ref: 72960; http://n2t.net/addgene:72960, Watertown, United States) via Golden Gate cloning and then Sanger sequenced (Macrogen Inc., Seoul, South Korea). The *rbcL* sequences (GenBank Accessions OP515528–OP515532) were translated and the RbcL peptides aligned using MEGAX ([Kumar et al., 2018](#)).

Statistical analysis

Differences among means were tested using one-way analysis of variance (ANOVA), after normality (Anderson–Darling test) and homogeneity of variances (Bartlett test) of the data were confirmed. Post-hoc comparisons were performed using Duncan test. For nonparametric data, Kruskal–Wallis test followed with Bonferroni correction was used. Pearson correlation coefficients were obtained for the significance of the association between different variables. P-values < 0.05 were considered significant. Data were analyzed using R

(version 3.2.3, 2015-12-10) with Rstudio interphase (RStudio Version 0.99.879—2009–2016, Inc.) and plotted using the ggPlot2 package (ggPlot2 version 2.2.1; Springer-Verlag New York, 2009–2016).

Supplemental data

The following materials are available in the online version of this article.

Supplemental Table S1. Description of the RbcL amino acid changes detected among the *Posidonia* species.

Supplemental Table S2. Parameters obtained from photosynthesis versus DIC (P–C) curves.

Supplemental Table S3. Biochemical leaf parameters.

Supplemental Table S4. Environmental variables of the sampling sites.

References

Agawin NSR, Ferriol P, Cryer C, Alcon E, Busquets A, Sintes E, Vidal C, Moyà G (2016) Significant nitrogen fixation activity associated with the phyllosphere of Mediterranean seagrass *Posidonia oceanica*: first report. Mar Ecol Prog Ser **551**: 53–62

Aigner H, Wilson RH, Bracher A, Calisse L, Bhat JY, Hartl FU, Hayer-Hartl M (2017) Plant RuBisCo assembly in *E. coli* with five chloroplast chaperones including BSD2. Science (80-) **358**: 1272–1278

Aires T, Marbà N, Cunha RL, Kendrick GA, Walker DI, Serrão EA, Duarte CM, Arnaud-Haond S (2011) Evolutionary history of the seagrass genus *Posidonia*. Mar Ecol Prog Ser **421**: 117–130

Badger MR, Andrews TJ, Whitney SM, Ludwig M, Yellowlees DC, Leggat W, Price GD (1998) The diversity and coevolution of Rubisco, plastids, pyrenoids, and chloroplast-based CO_2-concentrating mechanisms in algae. Can J Bot **76**: 1052–1071

Banda DM, Pereira JH, Liu AK, Orr DJ, Hammel M, He C, Parry MAJ, Carmo-Silva E, Adams PD, Banfield JF, et al. (2020) Novel bacterial clade reveals origin of form I Rubisco. Nat Plants **6**: 1158–1166

Bar-On YM, Milo R (2019) The global mass and average rate of Rubisco. Proc Natl Acad Sci USA **116**: 4738–4743

Bauwe H, Hagemann M, Kern R, Timm S (2012) Photorespiration has a dual origin and manifold links to central metabolism. Curr Opin Plant Biol **15**: 269–275

Bouvier JW, Emms DM, Rhodes T, Bolton JS, Brasnett A, Eddershaw A, Nielsen JR, Unitt A, Whitney SM, Kelly S (2021) Rubisco adaptation is more limited by phylogenetic constraint than by catalytic trade-off. Mol Biol Evol **38**: 2880–2896

Campey ML, Waycott M, Kendrick GA (2000) Re-evaluating species boundaries among members of the *Posidonia ostenfeldii* species complex (posidoniaceae) morphological and genetic variation. Aquat Bot **66**: 41–56

Cummins PL (2021) The coevolution of RuBisCO, photorespiration, and carbon concentrating mechanisms in higher plants. Front Plant Sci **12**: 662425

Davidi D, Shamshoum M, Guo Z, Bar-On YM, Prywes N, Oz A, Jablonska J, Flamholz A, Wernick DG, Antonovsky N, et al. (2020) Highly active Rubiscos discovered by systematic interrogation of natural sequence diversity. EMBO J **39**: 1–11

Du YC, Spreitzer RJ (2000) Suppressor mutations in the chloroplast-encoded large subunit improve the thermal stability of wild-type ribulose-1,5-bisphosphate carboxylase/oxygenase. J Biol Chem **275**: 19844–19847

Duarte CM (1991) Seagrass depth limits. Aquat Bot **40**: 363–377

Duarte CM, Chiscano CL (1999) Seagrass biomass and production: a reassessment. Aquat Bot **65**: 159–174

Duarte CM, Losada IJ, Hendriks IE, Mazarrasa I, Marbà N (2013) The role of coastal plant communities for climate change mitigation and adaptation. Nat Clim Chang **3**: 961–968

Fei C, Wilson AT, Mangan NM, Wingreen NS, Jonikas MC (2022) Modelling the pyrenoid-based CO_2-concentrating mechanism provides insights into its operating principles and a roadmap for its engineering into crops. Nat Plants **8**: 583–595

Flamholz AI, Prywes N, Moran U, Davidi D, Bar-On YM, Oltrogge LM, Alves R, Savage D, Milo R (2019) Revisiting trade-offs between rubisco kinetic parameters. Biochemistry **58**: 3365–3376

Fourqurean JW, Marbà N, Duarte CM, Diaz-Almela E, Ruiz-Halpern S (2007) Spatial and temporal variation in the elemental and stable isotopic content of the seagrasses *Posidonia oceanica* and *Cymodocea nodosa* from the Illes Balears, Spain. Mar Biol **151**: 219–232

Galmés J, Andralojc PJ, Kapralov MV., Flexas J, Keys AJ, Molins A, Parry MAJ, Conesa MÀ (2014a) Environmentally driven evolution of Rubisco and improved photosynthesis and growth within the C_3 genus *Limonium* (Plumbaginaceae). New Phytol **203**: 989–999

Galmés J, Capó-Bauçà S, Niinemets Ü, Iñiguez C (2019) Potential improvement of photosynthetic CO_2 assimilation in crops by exploiting the natural variation in the temperature response of Rubisco catalytic traits. Curr Opin Plant Biol **49**: 60–67

Galmés J, Kapralov MV, Andralojc PJ, Conesa MÀ, Keys AJ, Parry MAJ, Flexas J (2014b) Expanding knowledge of the Rubisco kinetics variability in plant species: environmental and evolutionary trends. Plant Cell Environ **37**: 1989–2001

Galmés J, Molins A, Flexas J, Conesa MÀ (2017) Coordination between leaf CO_2 diffusion and Rubisco properties allows maximizing photosynthetic efficiency in *Limonium* species. Plant Cell Environ **10**: 2081–2094

Garcias-Bonet N, Vaquer-Sunyer R, Duarte CM, Marbà N (2019) Warming effect on nitrogen fixation in Mediterranean macrophyte sediments. Biogeosciences **16**: 167–175

Gerlach JC, Cottier K (1974) The use of *Sorghums* as forage crops. Proc Agron Soc New Zeal **4**: 83–85

Giordano M, Beardall J, Raven JA (2005) CO_2 concentrating mechanisms in algae: mechanisms, environmental modulation, and evolution. Annu Rev Plant Biol **56**: 99–131

Goudet MMM, Orr DJ, Melkonian M, Müller KH, Meyer MT, Carmo-Silva E, Griffiths H (2020) Rubisco and carbon-concentrating mechanism co-evolution across chlorophyte and streptophyte green algae. New Phytol **227**: 810–823

Griffiths H, Meyer MT, Rickaby REM (2017) Overcoming adversity through diversity: aquatic carbon concentrating mechanisms. J Exp Bot **68**: 3689–3695

Hemminga MA, Duarte CM (2000) Seagrass Ecology. Cambridge University Press, Cambridge

Hermida-Carrera C, Kapralov MV, Galmés J (2016) Rubisco catalytic properties and temperature response in crops. Plant Physiol **171**: 2549–2561

Heureux AMC, Young JN, Whitney SM, Eason-Hubbard MR, Lee RBY, Sharwood RE, Rickaby REM (2017) The role of Rubisco kinetics and pyrenoid morphology in shaping the CCM of haptophyte microalgae. J Exp Bot **68**: 3959–3969

Iñiguez C, Capó-Bauçà S, Niinemets Ü, Stoll H, Aguiló-Nicolau P, Galmés J (2020) Evolutionary trends in Rubisco kinetics and their co-evolution with CO_2 concentrating mechanisms. Plant J **101**: 897–918

Iñiguez C, Galmés J, Gordillo FJL (2019) Rubisco carboxylation kinetics and inorganic carbon utilization in polar versus cold-temperate seaweeds. J Exp Bot **70**: 1283–1297

Invers O, Zimmerman RC, Alberte RS, Pérez M, Romero J (2001) Inorganic carbon sources for seagrass photosynthesis: an experimental evaluation of bicarbonate use in species inhabiting temperate waters. J Exp Mar Bio Ecol **265**: 203–217

Ishikawa C, Hatanaka T, Misoo S, Miyake C, Fukayama H (2011) Functional incorporation of *Sorghum* small subunit increases the catalytic turnover rate of Rubisco in transgenic rice. Plant Physiol **156**: 1603–1611

Kane H, Viil J, Entsch B, Paul K, Morell M, Andrews T (1994) An improved method for measuring the CO_2/O_2 specificity of ribulosebisphosphate carboxylase-oxygenase. Aust J Plant Physiol **21**: 449

Kapralov MV., Smith JAC, Filatov DA (2012) Rubisco evolution in C_4 eudicots: an analysis of amaranthaceae sensu lato. PLoS ONE **7**: e52974

Kiani-Pouya A, Rasouli F (2014) The potential of leaf chlorophyll content to screen bread-wheat genotypes in saline condition. Photosynthetica **52**: 288–300

Kim M, Brodersen KE, Szabó M, Larkum AWD, Raven JA, Ralph PJ, Pernice M (2018) Low oxygen affects photophysiology and the level of expression of two-carbon metabolism genes in the seagrass *Zostera muelleri*. Photosynth Res **136**: 147–160

Kumar S, Stecher G, Li M, Knyaz C, Tamura K (2018) MEGA X: molecular evolutionary genetics analysis across computing platforms. Mol Biol Evol **35**: 1547–1549

Lagriffoul A, Mocquot B, Mench M, Vangronsveld J (1998) Cadmium toxicity effects on growth, mineral and chlorophyll contents, and activities of stress related enzymes in young maize plants (*Zea mays* L.). Plant Soil **200**: 241–250

Larkum AWD, Davey PA, Kuo J, Ralph PJ, Raven JA (2017) Carbon-concentrating mechanisms in seagrasses. J Exp Bot **68**: 3773–3784

Larkum AWD, Orth RJ, Duarte CM (2006) Seagrass: Biology, Ecology and Conservation. Springer Netherlands, Dordrecht, Netherlands

Lavery PS, Mateo MÁ, Serrano O, Rozaimi M (2013) Variability in the carbon storage of seagrass habitats and its implications for global estimates of blue carbon ecosystem service. PLoS ONE **8**: e73748

Lewis E, Wallace D (1998) Program Developed for CO_2 System Calculations. Carbon Dioxide Information Analysis Center, Oak Ridge National Laboratory, US Department of Energy, Oak Ridge, Tennessee

Lichtenthaler H, Wellburn A (1983) Determinations of total carotenoids and chlorophylls *b* of leaf extracts in different solvents. Biochem Soc Trans **11**: 591–592

Lin MT, Orr DJ, Worrall D, Parry MAJ, Carmo-Silva E, Hanson MR (2021) A procedure to introduce point mutations into the Rubisco large subunit gene in wild-type plants. Plant J **106**: 876–887

Lin MT, Salihovic H, Clark FK, Hanson MR (2022) Improving the efficiency of Rubisco by resurrecting its ancestors in the family Solanaceae. Sci Adv **8**: 1–13

Maberly SC, Gontero B (2017) Ecological imperatives for aquatic CO₂-concentrating mechanisms. J Exp Bot **68**: 3797–3814

Mao Y, Catherall E, Díaz-Ramos A, Greiff GRL, Azinas S, Gunn L, McCormick AJ (2022) The small subunit of Rubisco and its potential as an engineering target. J Exp Bot 1–19, https://doi.org/10.1093/jxb/erac309

Martin-Avila E, Lim YL, Birch R, Dirk LMA, Buck S, Rhodes T, Sharwood RE, Kapralov MV., Whitney SM (2020) Modifying plant photosynthesis and growth via simultaneous chloroplast transformation of Rubisco large and small subunits. Plant Cell **32**: 2898–2916

Matsumura H, Shiomi K, Yamamoto A, Taketani Y, Kobayashi N, Yoshizawa T, Tanaka S, Yoshikawa H, Endo M, Fukayama H (2020) Hybrid rubisco with complete replacement of rice rubisco small subunits by *Sorghum* counterparts confers C₄ plant-like high catalytic activity. Mol Plant **13**: 1570–1581

Mazarrasa I, Marbà N, Garcia-Orellana J, Masqué P, Arias-Ortiz A, Duarte CM (2017) Effect of environmental factors (wave exposure and depth) and anthropogenic pressure in the C sink capacity of *Posidonia oceanica* meadows. Limnol Oceanogr **62**: 1436–1450

Morita K, Hatanaka T, Misoo S, Fukayama H (2014) Unusual small subunit that is not expressed in photosynthetic cells alters the catalytic properties of Rubisco in rice. Plant Physiol **164**: 69–79

Orr D, Alcântara A, Kapralov MV, Andralojc J, Carmo-Silva E, Parry MAJ (2016) Surveying Rubisco diversity and temperature response to improve crop photosynthetic efficiency. Plant Physiol **172**: 707–717

Price G., Badger M (1985) Inhibition by proton buffers of photosynthetic utilization of bicarbonate in *Chara corallina*. Aust J Plant Physiol **12**: 257–267

Raven JA, Beardall J (2014) CO₂ concentrating mechanisms and environmental change. Aquat Bot **118**: 24–37

Raven JA, Beardall J (2016) The ins and outs of CO₂. J Exp Bot **67**: 1–13

Raven JA, Beardall J, Sánchez-Baracaldo P (2017) The possible evolution and future of CO₂-concentrating mechanisms. J Exp Bot **68**: 3701–3716

Ricart AM, Ward M, Hill TM, Sanford E, Kroeker KJ, Takeshita Y, Merolla S, Shukla P, Ninokawa AT, Elsmore K, et al. (2021) Coast-wide evidence of low pH amelioration by seagrass ecosystems. Glob Chang Biol **27**: 2580–2591

Roberts DG, Moriarty DJW (1987) Lacunal gas discharge as a measure of productivity in the seagrasses *Zostera capricorni*, *Cymodocea serrulata* and *Syringodium isoetifolium*. Aquat Bot **28**: 143–160

Sage RF, Sage TL, Kocacinar F (2012) Photorespiration and the evolution of C₄ photosynthesis. Annu Rev Plant Biol **63**: 19–47

Satagopan S, Huening KA, Tabita FR (2019) Selection of cyanobacterial (*Synechococcus* sp. strain PCC 6301) rubisco variants with improved functional properties that confer enhanced CO₂-dependent growth of Rhodobacter capsulatus, a photosynthetic bacterium. Mol Biol Physiol **10**: 1–14

Savir Y, Noor E, Milo R, Tlusty T (2010) Cross-species analysis traces adaptation of Rubisco toward optimality in a low-dimensional landscape. Proc Natl Acad Sci USA **107**: 3475–3480

Serrano O, Lavery PS, López-Merino L, Ballesteros E, Mateo MA (2016) Location and associated carbon storage of erosional escarpments of seagrass *Posidonia* mats. Front Mar Sci **3**: 1–7

Serrano O, Lavery PS, Rozaimi M, Mateo MÁ (2014) Influence of water depth on the carbon sequestration capacity of seagrasses. Glob Biogeochem Cycles **28**: 950–961

Sharwood RE, Von Caemmerer S, Maliga P, Whitney SM (2008) The catalytic properties of hybrid Rubisco comprising tobacco small and sunflower large subunits mirror the kinetically equivalent source rubiscos and can support tobacco growth. Plant Physiol **146**: 83–96

Sharwood RE, Ghannoum O, Kapralov MV., Gunn LH, Whitney SM (2016) Temperature responses of Rubisco from Paniceae grasses provide opportunities for improving C₃ photosynthesis. Nat Plants **2**: 1–9

Sharwood RE, Sonawane BV., Ghannoum O (2014) Photosynthetic flexibility in maize exposed to salinity and shade. J Exp Bot **65**: 3715–3724

Spreitzer RJ, Peddi SR, Satagopan S (2005) Phylogenetic engineering at an interface between large and small subunits imparts land-plant kinetic properties to algal Rubisco. Proc Natl Acad Sci USA **102**: 17225–17230

Tcherkez GGB, Farquhar GD, Andrews TJ (2006) Despite slow catalysis and confused substrate specificity, all ribulose bisphosphate carboxylases may be nearly perfectly optimized. Proc Natl Acad Sci USA **103**: 7246–7251

Whitney SM, Baldet P, Hudson GS, John Andrews T (2001) Form I Rubiscos from non-green algae are expressed abundantly but not assembled in tobacco chloroplasts. Plant J **26**: 535–547

Whitney SM, Sharwood RE (2014) Plastid transformation for Rubisco engineering and protocols for assessing expression. Methods Mol Biol **1132**: 245–262

Whitney SM, Sharwood RE, Orr D, White SJ, Alonso H, Galmés J (2011) Isoleucine 309 acts as a C₄ catalytic switch that increases ribulose-1,5-bisphosphate carboxylase/oxygenase (Rubisco) carboxylation rate in *Flaveria*. Proc Natl Acad Sci USA **108**: 14688–14693

Young JN, Heureux AMC, Sharwood RE, Rickaby REM, Morel FMM, Whitney SM (2016) Large variation in the Rubisco kinetics of diatoms reveals diversity among their carbon-concentrating mechanisms. J Exp Bot **67**: 3445–3456

Zhu XG, Portis AR, Long SP (2004) Would transformation of C₃ crop plants with foreign Rubisco increase productivity? A computational analysis extrapolating from kinetic properties to canopy photosynthesis. Plant Cell Environ **27**: 155–165